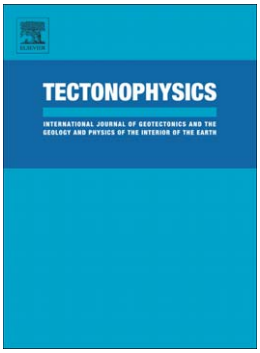

Seismic potential in the Italian Peninsula from integration and comparison of seismic and geodetic strain rates

Carmelo Angelica, Alessandro Bonforte, Giovanni Distefano, Enrico Serpelloni, Stefano Gresta

PII: S0040-1951(13)00455-1
DOI: doi: 10.1016/j.tecto.2013.07.014
Reference: TECTO 125976

To appear in: *Tectonophysics*

Received date: 28 December 2012
Revised date: 11 July 2013
Accepted date: 14 July 2013

Please cite this article as: Angelica, Carmelo, Bonforte, Alessandro, Distefano, Giovanni, Serpelloni, Enrico, Gresta, Stefano, Seismic potential in the Italian Peninsula from integration and comparison of seismic and geodetic strain rates, *Tectonophysics* (2013), doi: 10.1016/j.tecto.2013.07.014

Seismic potential in the Italian Peninsula from integration and comparison of seismic and geodetic strain rates.

Angelica Carmelo[(1)], Bonforte Alessandro[(2)], Distefano Giovanni[(1)], Serpelloni Enrico[(3)], Gresta Stefano[(1)]

(1) Università degli Studi di Catania, Dipartimento di Scienze Biologiche, Geologiche ed Ambientali, Corso Italia 55, 95129 Catania (Italy)

(2) Istituto Nazionale di Geofisica e Vulcanologia, Osservatorio Etneo, Piazza Roma 2, 95123 Catania (Italy)

(3) Istituto Nazionale di Geofisica e Vulcanologia, Centro Nazionale Terremoti, via D. Creti 12, 40128 Bologna (Italy)

Corresponding author: Alessandro Bonforte, Istituto Nazionale di Geofisica e Vulcanologia, Osservatorio Etneo, Piazza Roma 2, 95123 Catania (Italy), ph: +39-095-7165800, Fax: +39-095-7165826; alessandro.bonforte@ct.ingv.it

Abstract

Seismological and geodetic data provide key information about the kinematics and active tectonics of plate margins. Focal solutions enable determining the directions in which the current tectonic stress acts when fault rupturing occurs; GPS measurements provide information on the crustal velocity field and on current interseismic strain rates. The comparison of the strain rates resulting from the two datasets provides further insight into how large an area is affected by aseismic deformation, which is a valuable indicator for seismic hazard mitigation and estimating the seismic potential. In this work, we investigate both seismic and geodetic strain rates and the combined field resulting from the joint inversion of the geodetic and seismic datasets, providing a picture of the overall deformation field and its variation during the last decades. In this way, we seek to give an overview of the seismic potential distribution across the Apennines and southern Italy, as a qualitative analysis of space-time variations in the released seismic strain rate, compared to the space-time distribution of the cumulated geodetic strain rate. The results show a variable distribution of the seismic efficiency over the peninsula. The Southern Apennines shows the greatest seismic potential, highlighting a significantly lower seismicity in the last two decades over an area affected by the highest total strain rates. The Messina Straits and eastern Sicily have a significant seismic potential, together with the Calabrian arc (from the Tindari-Letojanni and central Aeolian islands to the Mt. Pollino area), as a result of seismic gaps with

respect to the combined strain rates in the investigated period. This long gap highlights the longer recurrence periods for the strongest earthquakes on this area. The central-northern Apennines and off-shore northern Sicily, show a lower seismic potential than central-southern Apennines, probably due to the more recent seismicity affecting these areas.

1. Introduction

The collision of the Adriatic Plate with the European continent closed the Tethys in the Mediterranean central region, giving rise to the Alps orogenic chain. Other microplates trapped between the two major ones (African and European) caused the formation of the complex arrangement of European mountain chains generally oriented east-west, while in the Middle East the Arabic Plate collided with Asia (Dewey et al., 1973; Le Pichon et al., 1988).

Over the past 30-35 My the Central and Western Mediterranean tectonics have been controlled by a retreating subduction inside the Africa-Europe convergence zone, with a roll-back and retreat of the subducting slabs (Dewey et al., 1989; Faccenna et al., 2001; Billi et al., 2011).

In the last 8 My, Ionian slab roll-back led to the opening of the Tyrrhenian Sea between the Corsica-Sardinia block and the Italian peninsula, due to the decoupling of the Calabro-Peloritani segment of the orogenic chain from the Corsica-Sardinia block and its migration south-eastwards to its present position. Here it docked 1-0.5 Ma, to become the toe of Italy and the eastern tip of Sicily. It is often assumed that

the roll-back and the accompanying back-arc extension continue until today. However, recent GPS observations (Hollenstein et al., 2003; Pondrelli et al., 2004; Devoti et al., 2011) in combination with neotectonic data, show that a tectonic reorganization must have occurred 1-0.5 Ma (Goes et al., 2004). Around 0.5 My ago, the compression between Africa and Europe was transferred from within Sicily to its northern off-shore (Goes et al., 2004).

A complex deformation zone now links the Sicilian back-thrust with the Calabrian part of the plate boundary, and further readjustments may still be occurring (Faccenna et al., 2001). This change in plate motions is most likely to be the response to the on-going collision with the irregular African margins in Sicily and Apulia (Goes et al., 2004).

Within this area, the Italian peninsula is the result of a complex geodynamic evolution and is now characterized by a set of different crustal blocks trapped between the Eurasian and African rigid plates (Fig. 1), whose kinematic and lateral variation in thickness and rheological parameters, make the convergence zone fragmented and irregularly shaped (Grasso, 2001).

Italian seismicity (http://csi.rm.ingv.it/) can be considered as superficial, since the hypocenters are concentrated at depths less than 50 km except in the area beneath the Calabrian arc, affected also by a deeper seismicity that reveals the presence of a subduction zone along a NW-dipping Benioff plane (Chiarabba et al., 2005).

The Italian peninsula has been affected by several destructive earthquakes that caused considerable loss of life and damage to human settlements. These events may strike

infrastructures and urban settlements, much larger today than in the past, with a significant risk to the inhabitants and/or integrity of infrastructures. Knowledge on the seismic history of Italy is limited to the period after the first millennium while, for more ancient times, there is no reliable information. After the first millennium, this history is marked by many earthquakes, of which the largest occurred in the Apennines, in Calabria and Eastern Sicily (Boschi et al., 1995 and 1997, http://emidius.mi.ingv.it/CPTI/home.html).

In this work, we modeled detailed seismic and geodetic strain rates field for Italy, allowing an improved interpretation of the current tectonics. Integration of the recent GPS information with seismicity data enables defining the deformation styles of the study region in detail; furthermore, we calculated the seismic efficiency distribution (i.e. seismic/geodetic strain rate ratio; Masson et al., 2005) over the entire area and also investigated its variation during the last decade. In this way, we can detect the most "potentially seismic" areas over the Apennines, by performing an analysis of space-time variations in the released seismic strain rate, compared to the space distribution of the cumulated geodetic strain rate.

2. Seismic Potential

Traditionally, seismic potential, namely the capacity of an area to generate earthquakes, is estimated from seismicity catalogs (Jenny et al., 2006). Using this approach, the southern Apennines, Calabrian arc, the Messina Straits and

southeastern Sicily have all been identified as high seismic hazard regions (e.g., Slejko et al., 1998, 1999; Brancato et al., 2009). Also the northern Apennines and western Sicily (Belice valley) are classified as areas with significant seismic hazard.

Seismic moment rate is proportional to seismic strain rates, thus allowing a comparison with other types of strain rate data (Jenny et al., 2006). It has been shown that instrumental seismicity catalogs, which are usually much shorter for Italy than the largest-event recurrence times, generally underestimate long-term average seismic moment rates (Ward, 1998; Jenny et al., 2004). This implies that Italy's instrumental seismic catalog most likely provides a lower limit for long-term average seismic strain rates, and for seismic potential estimations.

In this study, we use the information from geodetic data to calculate tectonic strain rates with the aim of improving seismic potential estimates for Italy. Assuming that tectonic loading (thus the slow overall deformation) is stationary in time, long-term average seismic strain rate release cannot exceed tectonic loading rates; conversely, it can be significantly lower, if part of the deformation occurs as aseismic creep or if elastic energy has not yet been released.

Seismic moment release estimates by Westaway (1992) (from macroseismic intensities of historical earthquakes) are comparable to geodetically measured strain rates in the Apennines (Hunstad et al., 2003), indicating that the deformation there has been entirely released by seismic activity. However Pondrelli (1999), using regional moment tensors, found that seismicity accounts for only about 30% of the total deformation inferred from VLBI data, along the Apennines, and for about 30%

in Calabria and 10% in Sicily. Only in the Sicily Channel, the estimated ratios reach a higher value (79%). Ward (1998) calculated similar low percentages by his comparison of seismic and VLBI strain rates. He attributed these low ratios to the short catalog length, compared to the long seismic cycle in this slowly deforming region. The rates comparison performed by Boschi et al. (1995) yields a very low 20-year probability of $M \geq 6$ crustal seismic event in most of Italy, except in northern and southeastern Sicily, where probabilities reach 65% along the northeastern coast.

These previous studies are significantly hampered by the sparse distribution of geodetic data. Here, we provide much more detailed strain rate fields for the Apennines and southern Italy, allowing an improved interpretation of the current active crustal deformation. In addition, by GPS and seismicity data combination we can provide a detailed distribution of the overall deformation styles over the region, and we can also calculate the seismic efficiency distribution (as the ratio between seismically released and cumulated geodetic deformation) over the entire area, investigating also its variation during the last decades. In this way, we try to provide a picture of the seismic potential distribution over the Apennines and southern Italy, as a qualitative analysis of space-time variation of the released seismic strain rate, compared to the space-time distribution of the cumulated geodetic strain rate.

3. Data sources

3.1 GPS data

In 1987, the first GPS survey across the Messina Straits was performed with single frequency receivers, over the terrestrial network of Caputo et al. (1981). The same network, with some additional TyrGeoNet stations (Anzidei et al., 2001), was re-occupied with dual frequency GPS receivers in 1994, partially in 2002 and 2004, and most recently in 2008 (Margheriti et al., 2008).

Following the December 13th 1990 earthquake in south-eastern Sicily, a first GPS network was installed around the epicentral area and surveyed in 1991. The former GPS network was later extended and currently consists of 50 stations. In 1998 and 2000, two GPS surveys were carried out on 26 stations of the northern half of network (Bonforte et al., 2002), and the same network was resurveyed more recently in 2006, also improving its geometry and logistics.

In this work, we analyze raw GPS data from several continuously operating GPS networks in Italy and surrounding regions, together with data from survey-mode GPS networks in Sicily (see Serpelloni et al, 2005, 2010 and Bonforte et al., 2002 for more details on the non-permanent networks). Most of the continuous GPS stations used belong to the INGV-RING network (Avallone et al., 2010). GPS velocities are obtained adopting a three-step approach (as in Serpelloni et al. 2006, 2010), including 1) raw phase data reduction, 2) combination of loosely-constrained solutions and reference frame definition, and 3) time-series analysis.

In the first step, we used daily GPS phase observations to estimate site position, adjustments to satellite orbital parameters, Earth orientation parameters, and time variable piecewise linear zenith and horizontal gradient tropospheric delay parameters

by means of the GAMIT software, version 10.4 (Herring et al., 2010), applying loose constraints to geodetic parameters. We processed all the data in the Euro-Mediterranean region together with data from networks operating in Africa and surrounding regions. Given the large number of sites, we broke the data down into several (>60) ~40-station subnets, and resolved integer phase ambiguities within each subnet. All regional subnets, including survey-mode networks, share a set of high quality IGS or regional stations, which are subsequently used as tie-stations during the combination in step 2). We applied the ocean-loading and a pole-tide correction model FES2004 (Lyard et al., 2006), and used the parameterized version of the VMF1 mapping function, the GMF (Boehm et al., 2006) for both hydrostatic and non-hydrostatic components of the tropospheric delay model. We used IGS absolute antenna phase center models for both satellite and ground-based antennas.

In the second step, we used the ST_FILTER program of the QOCA software (http:// http://qoca.jpl.nasa.gov) to combine our regional daily loosely-constrained solutions with the global solutions made available by SOPAC (http://sopac.ucsd.edu), and simultaneously created a global reference frame by applying generalized constraints. Specifically, we defined the reference frame by minimizing the velocities of the IGS global core stations (http://igscb.jpl.nasa.gov), while estimating a seven-parameter transformation with respect to the ITRF2008 NNR frame (Altamimi et al., 2011).

In the third step, we analyzed the position time-series, defined in the ITRF08 reference frame, with a least-squares method, in order to estimate station velocities.

Specifically, changes in station positions are modeled using the following functional model, where the position of a point x is given by:

$$x(t) = x_0 + bt + \alpha \cdot \sin(\omega t + \varphi) + \sum_{j=1}^{n} \Delta x_j H(t_j) \quad (1)$$

where t is the time, x_0 is the initial position bias, b is the secular rate, α and φ are the amplitude and phase, respectively, of the annual and semi-annual seasonal signals, H is the Heaviside step-function used to define coordinate jumps (Δx) at a given time t_j. Position outliers are cleaned from the time-series adopting a post-fit RMS criteria (values larger than 3 times the post-fit Weighted Root Mean Square, WRMS, are discarded). For the survey-mode data, we only fit the linear trend to the position time-series.

Only those stations having a minimum length of 2.5 years were retained in the subsequent analyses and the velocity field, thus avoiding biased velocities due to unreliable estimated seasonal signals (Blewitt and Lavallée, 2002) and underestimated velocity uncertainties due to absorbed correlated noise content in estimated trends of short time series (Williams et al., 2004).

Realistic velocity uncertainties were evaluated adopting a white- plus-colored noise model following the maximum likelihood estimation (MLE) approach implemented in the CATS software (Williams et al., 2004), and the procedures described in (Williams, 2003). In particular, for cGPS stations we adopted a white + flicker noise model, whereas for sGPS stations we adopted an error model that combines white + random walk noise using a value of 1 mm/yr0.5 for the random walk component (Hammond and Thatcher, 2004; Langbein and Johnson, 1997; Dixon et al., 2000, Beavan et al., 2002).

We used velocities and uncertainties of cGPS stations located on tectonically stable domains of the Eurasian plate in order to estimate their Euler rotation vectors with respect to the ITRF08 frame. Fig. 2 displays horizontal velocities with respect to the Eurasian fixed frame for GPS stations in the study area.

The reliability of the residual velocities is in very good agreement with other recent geodetic studies in this area (Serpelloni et al., 2005).

The geodetic dataset used for this work as input for the strain rates inversion procedures, is provided as auxiliary material (GPS.dat file).

3.2 *Focal Mechanisms of earthquakes*

A diffuse seismicity affects the entire Italian peninsula, with low-to-moderate magnitude earthquakes, mainly concentrated along the Apennines ridge (Fig. 3).

The seismology Group of the Harvard University systematically determine the focal parameters of the seismic sources for earthquakes with Ms>5 since 1977 using the "Centroid Moment Tensor" (CMT) method by inverting long periods body or mantle waves, according to the technique of Aki and Richards (1980). The catalog, available at www.seismology.harvard.edu/CMTsearch.html covers only a small portion of the recurrence time of events with major magnitude (M>=7), then it is down-sampled with respect to a whole seismic cycle for Italy; it therefore does not reflect the long-term seismic deformation, though it does provide important information on the geometry and orientation of the seismogenic structures.

To attain a more complete estimation of the seismic deformation of the Italian area, the contribution of smaller events, not included in the Harvard catalog, is also important; these reflect local variations of stress and/or originate from structures already present and reactivated such as an area of weakness. In the Mediterranean area, the Regional Centroid Moment Tensor (RCMT; Pondrelli et al., 2002, 2004) is calculated using surface waves for earthquakes with intermediate magnitude ($4.5<M<5.5$) recorded from 1997 by stations of the MEDiterranean NETwork (MEDNET; Boschi et al., 1991) and by other seismic networks. The Italian CMT dataset results from the collection of all centroid moment tensors computed for the Italian region for the entire period of available digital seismic data, i.e. from 1977 to present.

Surface waves (inverted to compute RCMTs) have a better signal-to-noise ratio at regional distance than long period body or mantle waves at global distance (inverted to compute CMTs), so the RCMT method seems more appropriate to study smaller magnitude seismic sources.

In this study, moment tensor solutions are taken from the Italian CMT dataset (www.bo.ingv.it/RCMT/Italydataset.html), for events with $M \geq 4.0$ and depth ≤ 30 km; the focal mechanisms used to constrain the style of seismic strain are shown in Fig.4. This magnitude threshold ensures inputting only good quality focal mechanisms, allowing reliable seismic strain tensor estimations.

The seismic dataset used for this work as input for the strain rates inversion procedures, is provided as auxiliary material (earthquakes.dat file).

4. Strain fields

Seismological and geodetic data provide important information on the kinematics and active tectonic of plate margins. The focal mechanisms alone allow determining the directions in which the current tectonic stress acts when fault rupturing occurs; GPS measurements alone give information on the overall crustal velocity field (Fig. 5a) and current interseismic strain rates. It should be remembered that the data obtained from the two methodologies can only be compared assuming that the strain rate remains constant over the study area for a long time and the comparison is made over an area several times larger than the seismogenic thickness (Jenny et al., 2006).

This study involved the Italian area from the northern Apennines to Sicily, excluding those areas affected by active volcanism.

Both strain rate fields (geodetic and seismic) were modeled using the method of Haines and Holt (Haines and Holt, 1993; Holt and Haines, 1995; Haines et al., 1998; Beavan and Haines, 2001). Following this method, we adopted a spherical geometry, expressed in terms of a rotation function W(r) by using a bi-cubic Bessel interpolation on a regular grid (Haines et al., 1998) with a variable spacing of knot points. In order to overcome the underestimation of the seismicity due to the short record of the seismic catalogues with respect to the mean recurrence times of the strongest

earthuakes, an "incompleteness factor" (also called "missing earthquake") is considered in the calculation according to the procedure used by Haines et al. (1998).

In calculating the deformation fields, the choice was made to apply a light smoothing, repeating the procedure once. This choice is primarily dictated by the particular feature of the Italian area where significant lateral variation between different deformation styles, would have been attenuated applying a greater smoothing factor.

4.1 Geodetic strain rates

Inversion of the horizontal geodetic velocities (Fig. 5b) reveals a strain rate field that, along the Apennines, has an extensional regime characterized by a generally clockwise rotation of the extension axes, following the chain axis, from the northern Apennines to the Calabrian arc; direction of the extension axes changes from N67°E to N130°E from Latitude 41.5° to 39.0°. The south-Tyrrhenian area is affected by predominant contraction extending from the Sardinia Channel to the Aeolian Is. and presenting, in the eastern sector, an extensional component showing a similar rotation to the one described for the Apennines. The intensity of crustal deformation is lower in central Sicily, Puglia and the central-northern Apennines, where the lack of GPS stations reduces the reliability of the geodetic strain rate field, and according to the rigid-like behavior of these microplates (e.g., Serpelloni et al., 2010).

This strain rate field (Fig. 5b) seems to concur well with the structural-geological data of literature (Monaco and Tortorici, 2000; Catalano et al., 2008).

4.2 Seismic strain rates

In Fig. 6, showing the results of the seismic strain rates analysis, we note that the general seismic deformation rate is much lower than the geodetic one; this feature has also been observed by a similar previous analysis (Jenny et al., 2006) and it may likely be due to the fact that only a fraction of the elastic energy accumulated by the rocks is released by seismic release in the interval covered by the seismic catalogue used here. Besides the absolute values, as it is usually done in literature, it is interesting to analyze the pattern of the seismic strain tensors distribution over the study area.

The seismic strain analysis provides a strain pattern that is in good agreement with the structural-geological data and geodetic data, showing how the seismic deformation is mainly distributed in the neighborhood of the main seismotectonic structures.

The seismic strain rate field obtained in the southern-central Apennines area (Fig. 6) shows a prevailing extensional system, NE-SW oriented. Southwards, through the Calabrian arc down to the Hyblean-Maltese Escarpment, the seismic deformation style shows a transition to a prevailing compressional regime, with NNW-SSE oriented contraction axes on northern Sicily and its off-shore.

5. Combined strain field

Considering that the geodetic strain takes into account the whole crustal deformation, while the seismic strain takes into account only the deformation released during fault ruptures, we applied the same method to perform a joint inversion of seismic and geodetic data, automatically calculating Kostrov's summation with GPS observation constraints. In this way, we combined the total deformation rates recorded by GPS networks from 1990 to 2009 to the seismic one recorded from 1976 to 2009. This combination allows estimating longer-term total strain tensors (for the longest interval available, 1976-2009), investigating a period that better fits the recurrence times of some earthquakes in the peninsula.

A variable distribution of the deformation rates is evident on observing the combined strain map for the Italian peninsula (Fig. 7); these results well fit the known geological-structural framework. This integrated strain field is the most constrained result, taking into account all the available information, and it depicts the active tectonic framework and the current deformation of the peninsula fairly accurately. It is affected by a dominant NE-SW extension along the NW-SE Apennines ridge, with higher values on its central-northern and, especially, southern parts. The two sectors of the Apennines chain are separated by a central part where dextral shear strain rates predominate along an E-W direction, compatible with the kinematics of the eastern Molise – Mattinata fault zone systems (MF in Fig. 7) in the Gargano promontory area (Di Bucci et al., 2010). On the southernmost part of the peninsula, strain rates rapidly decrease across the Mt Pollino zone and much lower strain rates affect the entire Calabrian arc. The Messina Straits shows a WNW-ESE extension accompanied by a

minor but significant orthogonal contraction; here, the strain rates may be the result of the extension controlling the NE-SW normal fault system of the Messina Straits graben, but also of the dextral shear affecting the NNW-SSE Tindari-Letojanni fault system (TL in Fig. 7) cutting NE Sicily (Billi et al., 2006). A NNW-SSE contraction with a significant shear strain component affects a wide area on the southern Tyrrhenian Sea extending to inland in northern Sicily, and involving the western branch of the Aeolian archipelago. Along the central branch of the archipelago, the contraction rotates to roughly NNE-SSW with a shear component compatible with a transpressive dextral kinematics along a NNW-SSE structure (according to Bonforte and Guglielmino, 2008). East of the central segment of the Aeolian archipelago, strain tensors change to a main NW-SE extension related to the back arc extension of the Calabrian.

6. Discussion

Seismic and geodetic data were exploited to produce two different maps of strain rates distribution. A combination of the two strain rates data was then made in order to take advantage of the different information coming from the two datasets. The crustal velocity field immediately reveals a NE-wards motion of the entire Adriatic sector of the Apennines chain (Fig. 5a), while relative stability characterizes all stations along the western coast of the peninsula. In Sicily, a rotation of station velocities is evident,

changing from the NE-wards motion on the Messina Straits to a NNW-wards motion in western and south-eastern Sicily.

These features produce a significant NE-SW geodetic extension (Fig. 5b) along the entire peninsula, with the higher values in the northern and southern parts of the chain, coupled with a significant NW-SE contraction in the Gargano area and at the north-western tip of the chain, producing a dominant shear-strain regime with a dominant roughly N-S contraction on the northern border of the area studied in this work. Rotation and divergence of the station velocities across the Messina Straits result in a NW-SE extension, while in eastern Sicily it is again oriented NE-SW. In the northern off-shore of Sicily, the decrease of GPS velocities along the southern Tyrrhenian sea produces a N-S oriented contraction. This strain distribution concurs well with the distribution of seismicity in Italy (Figs. 3 and 4). Indeed, most of the M>4 events affect the central-northern and southern Apennines, mainly with normal kinematics along NW-SE oriented fault planes; some strike slip mechanisms affect the areas where also geodetic shear strain was found (in the Gargano area and at the northernmost part of the Apennines). This agreement is evident when comparing the geodetic (Fig. 5b) and seismic (Fig. 6) strain rates tensors. The seismic strain distribution highlights that a significant seismic deformation affected mainly the central-northern and southern Apennines (from 1976 to 2009). Lower seismic deformation rates have been found on the rest of the peninsula (northernmost part of Apennines, Calabrian arc and Messina Straits).

The joint inversion of geodetic and seismic strain rates (Fig. 7) defines the most constrained pattern of the overall deformation styles and rates affecting the peninsula from 1976 to 2009 (taking into account the seismic rupture styles and the "total" geodetic deformation) and allows its active tectonic framework to be finely depicted. - The map in Fig. 7 evidences important heterogeneities in the distribution of the deformation, identifying three main areas showing different and peculiar features: central-northern Apennines, southern Apennines and Calabrian arc – Sicily. In the following, we define the 1976-2009 total strain rates (resulting from the combined inversion) as "long-term", in order to differentiate them from the 1990-2009 "short-term" total strain rates (coming from geodetic data inversion).

6.1 Central-northern Apennines

This area shows significant combined strain rates over the 1976-2009 interval (Fig. 8a); a NE-SW extension affects the entire northern Apennine ridge, gradually decreasing only on the north-westernmost tip of the chain; this area was affected by important seismicity in September 1997 (M_{max}=6.0, the "Colfiorito earthquake") and by the more recent destructive sequence that struck central Italy in April 2009 (the "Aquila sequence"), reported as stars in Fig. 8b and 8c. These events released most of the deformation accumulated on the faults, as revealed by the important strain rates resulting from considering only the seismic data for the same 1976-2009 interval and reported for comparison in Fig. 8b. This aspect is more evident by the contouring of

the seismic efficiency (reported in Fig. 8b as the ratio between the seismic and geodetic maximum shear strain for 1976-2009 at each cell of the grid, in percent), showing the highest values in the central-northern part of the Apennines and the very low seismic release in the northernmost part.

Indeed, in the northernmost part of the peninsula, significant total strain rates do not correspond to proportionate seismic strain rates (that are almost null), evidencing a probable spatial gap in the seismic release distribution. In order to evaluate an eventual recent variation in the rates of the seismic strain release, we calculated shorter-period strain rates and seismic efficiency considering the seismic data recorded in the 1990 to 2009 interval (Fig. 8c), consistent with the time span of geodetic data (Fig. 8d). In the northern Apennines, the short period comparison (Fig. 8c and 8d) does not indicate significant differences in the distribution of ratios between seismic and total strain rates with respect to the long period, increasing only the seismic efficiency in the areas close to the most significant recent seismic releases (due to the shorter time interval considered) and confirming the gap in the seismic release in the northernmost part.

6.2 Central-southern Apennines

The central-southern part of the Apennines, generally defined as a high risk area (Slejko et al., 1999), shows very high long-term total strain rates (Fig. 9a). This area is affected by a strong NE-SW extension where important seismic sequences have occurred in recent times, including the M=6.9 destructive earthquake in November 1980 (the “Irpinia earthquake”) and by an evident shear strain just northward, where a

M=5.7 event occurred on October 31, 2002 (the "S. Giuliano earthquake"), shown as stars in Fig 9b and 9c. Long-term seismic strain rates (Fig. 9b) show the same pattern as the combined ones, confirming that the deformation accumulated has been proportionally released by the seismicity occurring from 1976 to 2009, with the highest values of seismic efficiency around the area struck by the October 31 2002 event. Conversely, the short-term seismicity (Fig. 9c) shows an evident lack of seismic deformation in the southernmost part with respect to the long-term analysis, with a consequent drop in seismic efficiency for the 1990-2009 period. This is important evidence of a short-term seismic gap in the southern Apennines during the last two decades, indicating a significant re-charging of the structures that had already produced destructive earthquakes.

6.3 Calabrian Arc

In the southernmost end of the peninsula (Fig. 10a), lower combined strain rates have been detected for the 1976-2009 interval. Significant strain rates (even lower than on the Apennines) affect only the Messina Straits and northern Sicily, respectively with NW-SE extension and NNW-SSE compression. These areas were not affected by significant seismicity in recent times, though eastern Sicily has undergone the most catastrophic events in Italy. The Messina Straits was struck by a M 7.3 earthquake in 1908 (the "Messina earthquake") that destroyed Messina and Reggio Calabria also due to the subsequent tsunami. South-eastern Sicily, albeit not showing significant strain rates in this study, has been struck by several important seismic events in historical

times, the most important one being the 1693 earthquake (the "Val di Noto" earthquake) that destroyed Catania, Siracusa and Ragusa. For the whole considered period (1976-2009), there is only one recent important event (13/12/1990, M= 5.6) in this area, occurring in the Hyblean-Maltese Escarpment in the eastern off-shore of Sicily, where no geodetic information is available for estimating the seismic potential. The northern off-shore of Sicily was recently struck by only one major event of M=5.9 in September 2002 and smaller magnitude seismic sequences. The described recent seismic activity produced significant strain rates (Fig. 10b) only in the northern onshore and off-shore of Sicily, evidencing a long-term gap over the entire eastern part of the island with very low values of seismic efficiency. This gap is also confirmed by the short-term seismic strain rates (Fig. 10c) and it is even more evident if compared to the geodetic strain rates for the same time period (Fig. 10d).

Unfortunately, geodetic networks do not provide enough detail in the south-western part of Sicily, preventing a discussion for this seismic area.

By looking at the overall distribution of the seismic efficiency over the entire peninsula in the entire 1976-2009 interval (Fig. 11a), it is possible to detect the maximum seismic strain release across the eastern slopes of the central-southern Apennines and another relative maximum elongated along the ridge of the central-northern Apennines. By calculating the difference in the seismic efficiency between the two periods investigated (1976-2009 and 1990-2009, Fig. 11b), it is evident a significant decrease in the seismic release in the Tyrrhenian side of the southern

Apennines over the last two decades, while the rest of the peninsula shows no significant differences.

7. Conclusions

In this work, the geodetic and seismic strain over the Italian peninsula has been analyzed to investigate the rates and style of crustal deformation and integrated to evaluate the seismic potential.

The deformation rates obtained from seismic and geodetic data show the same style of deformation and a coherent kinematics in the areas where both datasets provide detailed information. In general, the entire Apennines are undergoing a NE-SW extension, orthogonal to the axis of the chain; the energy accumulated by this deformation is seismically released by the NW-SE oriented normal fault systems present all along the chain, as confirmed by seismic strain rates and focal solutions. An important shear zone has been detected by the geodetic strain analysis in the Gargano area, in good agreement with the seismic strain data and the focal solution of the recent earthquake. Contraction has been found along the northern off-shore of Sicily by both seismic and geodetic data.

The results show a variable distribution of the seismic potential, evaluated in terms of seismic efficiency over the peninsula for the 1976-2009 period at grid cell scale. The southern Apennines show the highest seismic potential; furthermore, comparisons between “long”- (1976-2009) and “short”- (1990-2009) term data,

reveal a decrease in the seismic efficiency over the last two decades along the southern Apennines, highlighting an important gap in the seismicity over an area affected by the highest total strain rates. Central-northern Apennines and northern off-shore of Sicily, show a lower seismic potential than the central-southern Apennines, also probably due to the more recent seismicity affecting these areas.

The Messina Straits and eastern Sicily show a significant seismic potential, together with the Calabrian arc (from the Tindari-Letojanni and central Aeolian islands to the Mt. Pollino area), due to seismic gaps in both short- and log-term analyses with respect to the total strain rates. This long gap evidences the longer recurrence periods for the strongest earthquakes in this area.

Acknowledgements

C. Angelica activity at INGV - Osservatorio Etneo was supported by a PhD grant by the Universtà di Catania. Authors want to thank all technicians of the INGV ground deformation group for their fundamental activities in field data collection by GPS surveys and for the availability of continuous data from permanent stations. Authors are indebted to S. Conway for his precious help in improving the English language of the early manuscript and to Philippe Vernant and anoother anonymous reviewer for their comments and suggestion that allowed us to significantly improve the paper.

References

Altamimi, Z., Collilieux, X., Métivier, L., 2011. ITRF2008: an improved solution of the international terrestrial reference frame, J. Geodesy 85(8), 457–473, doi:10.1007/s00190-011-0444-4.

Anzidei, M., Baldi, P., Casula, G., Galvani, A., Mantovani, E., Pesci, A., Riguzzi, F., Serpelloni, E., 2001. Insights into present-day crustal motion in the central Mediterranean area from GPS surveys. Geophys. J. Int. 146, 98-110.

Avallone, A. et al. (2010), The RING network: improvements to a GPS velocity field in the central Mediterranean, *Ann Geophys-Italy*, *53*(2), 39–54, doi:10.4401/ag-4549.

Beavan, J., Tregoning, P., Bevis, M., Kato, T., Meertens, C., 2002. Motion and rigidity of the Pacific Plate and implications for plate boundary deformation. J. Geophys. Res. 107, doi:10.1029/2001JB000282.

Billi, A., Barberi, G., Faccenna, C., Neri, G., Pepe, F., Sulli, A., 2006. Tectonics and seismicity of the Tindari Fault System, southern Italy: Crustal deformations at the transition between ongoing contractional and extensional domains located above the edge of a subducting slab. Tectonics, Vol. 25, TC2006, doi:10.1029/2004TC001763.

Billi A., Faccenna, C., Bellier, O., Minelli, L., Neri, G., Piromallo, C., Presti, D., Scrocca, D., Serpelloni, E., 2011. Recent tectonic reorganization of the Nubia-Eurasia convergent boundary heading for the closure of the western Mediterranean, *B Soc Geol Fr, 182(4), 279-303*.

Bonforte, A., Anzidei, M., Puglisi, G., Mattia, M., Campisi, O., Casula, G., Galvani, A., Pesci, A., Puglisi, B., Gresta, S., Baldi, P., 2002. GPS surveys in the foreland-foredeep tectonic system of Southeastern Sicily: first results. Ann. Geof. Vol. 45, N. 5, October 2002.

Bonforte , A., Guglielmino, F., 2008. Transpressive strain on the Lipari–Vulcano volcanic complex and dynamics of the “La Fossa” cone (Aeolian Islands, Sicily) revealed by GPS surveys on a dense network. Tectonophysics, doi:10.1016/j.tecto.2008.05.016.

Boschi, E., Giardini, D., Morelli, A., 1991. MedNet: the very broadband seismic network for the mediterranean. Il nuovo Cimento, 14, 7999.

Boschi, E., Gasperini, P., Mulargia, F., 1995. Forecasting where larger crustal earthquakes are likely to occur in Italy in the near future. Bull. Seismol. Soc. Am. 85 (5), 1475–1482.

Boschi E., Ferrari, G., Gasperini, P., Guidoboni, E., Valensise, G., 1997. Catalogo dei forti terremoti in Italia dal 461 a.c. al 1980. Istituto Nazionale di Geofisica, Roma.

Boehm J, Niell A, Tregoning P, Schuh H (2006), Global Mapping Func- tion (GMF): a new empirical mapping function based on numerical weather model data, *Geophys. Res. Lett.*, 33:L07304. doi:10.1029/2005GL025546.

Brancato, A., Hole, J., A., Gresta, S., Jacob, J., N., 2009. Determination of Seismogenic Structures in Southeastern Sicily (Italy) by High-Precision Relative Relocation of Microearthquakes. Bulletin of the Seismological Society of America, Vol. 99, No. 3, pp. 1921 – 1936, June 2009, doi: 10.1785/0120080204.

Caputo M., Pieri L., Barbarella M., Gubellini A., Russo P e Console R., 1981. Geophysical and geodetic observations in the Messina Straits, Tectonophysics, 74, 147-154.

Catalano S., De Guidi, G., Monaco, C., Torotrici, G., Tortorici, L., 2008. Active faulting and seismicity along the Siculo–Calabrian Rift Zone (Southern Italy). Tectonophysics, 453 (2008) 177–192.

Chiarabba, C., Jovane, L., Distefano, R., 2005. A new view of Italian seismicity using 20 years of instrumental recordings. Tectonophysics, 395, 251-268.

Devoti, R., Esposito, A., Pietrantonio, G., Pisani, A., R., Riguzzi, F., 2011. Evidence of large scale deformation patterns from GPS data in the Italian subduction boundary, *Earth and Planetary Science Letters*, *311*(3-4), 1-12, doi: 10.1016/j.epsl.2011.09.034.

Dewey, J., F., Pitman, W., C., Ryan, W., B., F., Bonnin, B., 1973. Plate tectonics and the evolution of the Alpine system, Bull. Soc. Am. Bull., 84, 3137– 3180.

Dewey, J., F., Helman, M., Turco, E., Hutton, D., Knott, S., 1989. Kinematics of the western Mediterranean. In: Coward, M., Dietrich, D., Park, R. (Eds.), Alpine Tectonics Spec. Publ. Geol. Soc., vol. 45. Blackwell Scientific Publications, London, pp. 265–283.

Di Bucci, D., Burrato, P., Vannoli, P., Valensise, G., 2010. Tectonic evidence for the ongoing Africa Eurasia convergence in central Mediterranean foreland areas: A journey among long lived shear zones, large earthquakes, and elusive fault motions. J. Geof. Research, VOL. 115, B12404, doi:10.1029/2009JB006480, 2010.

Dixon, T., H., Miller, M., Farina, F., Wang, H., Z., Johnson, D., 2000. Present-day motion of the Sierra Nevada block and some tectonic implications for the Basin and Range province, North American Cordillera. Tectonophysics, 19, 1–24.

Faccenna, C., Becker, T., W., Lucente, F., P., Jolivet, L., Rossetti, F., 2001. History of subduction and back-arc extension in the central Mediterranean. J. Geophys. Int. 145, 809–820.

Goes, S., Giardini, D., Jenny, S., Hollenstein, C., Kahle, H., G., Geiger, A., 2004. A recent tectonic reorganization in the South-Central Mediterranean. Earth Planet. Sci. Lett. 225, 335–345.

Grasso, M., 2001. The Appenninic-Magrebid orogen in southern Italy, Sicily and adjacent areas. In G.B. Vai and I.P.Martini (eds) Anatomy and Orogen: The Appennines adjacent Mediterranean Basins, 255247.

Haines, A., J., Holt, W., E., 1993. A procedure for obtaining the complete horizontal motions within zones of distributed deformation from the inversion of strain rate data. J. Geophys. Res. 98, 12057–12082.

Haines, A., J., Jackson, J., A., Holt, W., E., Agnew, D., C., 1998. Representing distributed deformation by continuous velocity fields. Sci. Rept. 98/5, Inst. of Geol. and Nucl. Sci. Wellington, New Zealand.

Hammond, W., C., Thatcher, W., 2004. Contemporary tectonic deformation of the Basin and Range province, western United States: 10 years of observation with the Global Positioning System. J. Geophys. Res. 109, B08403. doi:10.1029/2003JB002746.

Herring, T., King, R., W., McClusky, S., 2010. *GAMIT Reference Manual, Relese 10.4*, Massachussetts Institute of Technology, Cambridge, MA.

Hollenstein, C., Kahle, H., G., Geiger, A., Jenny, S., Goes, S., Giardini, D., 2003. New GPS constraints on the Africa–Eurasia Plate Boundary Zone in southern Italy. Geophys. Res. Lett. 30 (18), 1935. doi:10.1029/2003GL017554.

Holt, W., E., Haines, A., J., 1995. The kinematics of northern South Island, New Zealand, determined from geologic strain rates. J. Geophys. Res. 100, 17991–18010.

Hunstad, I., Selvaggi, G., D'Agostino, N., England, E., Clarke, P., Pierozzi, M., 2003. Geodetic strain in peninsular Italy between 1875 and 2001. Geophys. Res. Lett. 30 (4), 1181. doi:10.1029/ 2002GL016447.

Jenny, S., Goes, S., Giardini, D., Kahle, H., G., 2004. Earthquake recurrence parameters from seismic and geodetic strain rates in the eastern Mediterranean. Geophys. J. Int. 157, 1331–1347.

Jenny, S., Goes, S., Giardini, D., Kahle, H., G., 2006. Seismic potential of Southern Italy. Tectonophysics, 415 (2006) 81 – 101.

Langbein, J., Johnson, H., 1997. Correlated errors in geodetic time series: Implications for time-dependent deformation, J. Geophys. Res., 102, 591–603.

Le Pichon, X., Bergerat, F., Roulet, M., J., 1988. Plate kinematics and tectonics leading to the Alpine belt formation: a new analysis, Geol. Soc. Am., Spec. Pap., 218, 111–131.

Lyard, F., Lefevre, F., Letellier, T., Francis, O., 2006. Modelling the global ocean tides: modern insights from FES2004, Ocean Dynam., 56, 394-415.

Margheriti, L., Messina 1908-2008 Team, 2008. Understanding crust dynamics and subduction in southern Italy, Eos Trans. AGU, 89(25), 225–226.

Masson, F., Chèry, J., Hatzfeld, D., Martinod, J., Vernant, P., Tavakoli, F., Ghafory-Ashtiani, M., 2005. Seismic versus aseismic deformation in Iran inferred from earthquakes and geodetic data, J. Geophys. Int., 160, 217 – 226, doi: 101111/j.1365-246X.2004.02465.x.

Monaco, C., Tortorici, L., 2000. Active faulting in the Calabrian arc and eastern Sicily. J. Geodyn. 29, 407–424.

Pondrelli, S., 1999. Pattern of seismic deformation in the western Mediterranean. Ann. Geofis. 42 (1), 57–70.

Pondrelli, S., Morelli, A., Ekström, G., Mazza, S., Boschi, E., Dziewonski, E., A., M., 2002. European–Mediterranean regional centroid-moment tensors: 1997–2000. Phys. Earth Planet. Int. 130, 71–101.

Pondrelli, S., Piromallo, C., Serpelloni, E., 2004. Convergence vs. retreat in southern Tyrrhenian Sea: insights from kinematics. Geophys. Res. Lett. 31, L06611. doi:10.1029/2003GL019223.

Reilinger, R. et al. (2006), GPS constraints on continental deformation in the Africa-Arabia-Eurasia continental collision zone and implications for the dynamics of plate interactions, *J Geophys Res*, *111*(B5), doi:10.1029/2005JB004051.

Serpelloni, E., Anzidei, M., Baldi, P., Casula, G., Galvani, A., 2005. Crustal velocity and strain rate fields in Italy and surrounding regions: new results from the analysis of permanent and nonpermanent GPS networks. GJI 161 (3), 861–880.

Serpelloni, E., Casula, G., Galvani, A., Anzidei, M., Baldi, P., 2006. Data analysis of permanent GPS networks in Italy and surrounding regions: application of a distributed processing approach, *Ann Geophys.-Italy*, *49*, 897-928.

Serpelloni, E., Bürgmann, R., Anzidei, M., Baldi, P., Mastrolembo-Ventura, B., Ventura, Boschi, E., 2010. Strain accumulation across the Messina Straits and kinematic of Sicily and Calabria from GPS data and dislocation modeling, *Earth Planet. Sc. Lett.*, *298*(3-4), 347-360, doi: 10.1016/j.epsl.2010.08.005.

Slejko, D., Peruzza, L., Rebez, A., 1998. Seismic hazard maps of Italy. Ann. Geofis. 41, 183–214.

Slejko, D., Camassi, R., Cecic, I., Herak, D., Herak, M., Kociu, S., Kouskouna, V., Lapajne, J., Makropoulos, K., Meletti, C., Muco, B., Papaioannou, C., Peruzza, L., Rebez, A., Scandone, P., Sulstarova, E., Voulgaris, N., Zivcic, M., Zupancic P., 1999. GSHAP seismic hazard assessment for Adria. Ann. Geofis., GSHAP Spec. vol. 42 (6), 1085–1107.

Ward, S., N., 1998. On the consistency of earthquake moment release and space geodetic strain rates: Europe. Geophys. J. Int. 135, 1011–1018.

Westaway, R., 1992. Seismic moment summation for historical earthquakes in Italy: tectonic implications. J. Geophys. Res. 97, 15437–15464.

Williams, S., 2003. The effect of coloured noise on the uncertainties of rates estimated from geodetic time series, J. Geodesy, 76, 483–494, doi:10.1007/s00190-002-0283-4.

Williams, S., Bock, Y., Fang, P., Jamason, P., Nikolaidis, R., Prawirodirdjo, L., Miller, M., Johnson, D., 2004. Error analysis of continuous GPS position time series, J. Geophys. Res., 109, doi:10.1029/2003JB002741.

Figure Captions

Figure 1. Structural sketch map of Italian peninsula with main tectonic features. HME: Hyblean-Maltese escarpment; MS: Messina Straits.

Figure 2. GPS velocities and associated error ellipses for the entire Italian peninsula. Black arrows for permanent stations; gray arrows for surveys.

Figure 3. Distribution of Italian seismicity and major active faults. Gray dots, historical seismicity with MCS intensity > VII, (Parametric catalog of Italian earthquakes CPTI04 from 217 B.C. to 2002). Black dots, instrumental earthquakes with M>=3 and depth ≤30km, (Catalog of Italian seismicity CSI from 1981 to 2002). Major active faults from (http://ccgm.free.fr/mediterra_geodyn_gb.html).

Figure 4. Focal mechanism for M>=4.0 and depth <=30 km seismicity, considered for seismic strain rates calculation; (The Italian CMT dataset; http://www.bo.ingv.it/RCMT/Italydataset.html).

Figure 5. a) Crustal velocity field resulting from the inversion of GPS velocities and b) geodetic strain rates resulting by inverting the velocity pattern.

Figure 6. Seismic strain rates resulting from the inversion of focal mechanisms. Stars indicate the locations of the strongest earthquakes recorded during the investigated period.

Figure 7. Combined final strain rates resulting from joint inversion of GPS and seismic data. White arrows across dashed gray lines indicate the main extension areas; solid lines represent strike-slip faults in the most significant shear strain zones; dashed black line with converging black arrows indicates the compression

front of the chain in the Ionian sea; the gray shadowed area indicates a transpressive regime affecting the northern off-shore of Sicily. See text for more details.

Figure 8. Detail on the northern Apennines. **a)** combined strain rates from 1976 to 2009; **b)** seismic strain rates from 1976 to 2009; **c)** seismic strain rates from 1990 to 2009; **d)** geodetic strain rates from 1990 to 2009; contour in Figs. b and c, indicate seismic efficiency.

Figure 9. Detail on the southern Apennines. **a)** combined strain rates from 1976 to 2009; **b)** seismic strain rates from 1976 to 2009; **c)** seismic strain rates from 1990 to 2009; **d)** geodetic strain rates from 1990 to 2009; contour in Figs. b and c, indicate seismic efficiency.

Figure 10. Detail on the Calabrian arc and Sicily. **a)** combined strain rates from 1976 to 2009; **b)** seismic strain rates from 1976 to 2009; **c)** seismic strain rates from 1990 to 2009; **d)** geodetic strain rates from 1990 to 2009; contour in Figs. b and c, indicate seismic efficiency.

Figure 11. **a)** Contour of the distribution of the seismic efficiency over the peninsula plotted together with the focal solutions of the earthquakes inverted and **b)** contour of the differences between the 1976-2009- and 1990-2009 seismic efficiencies.

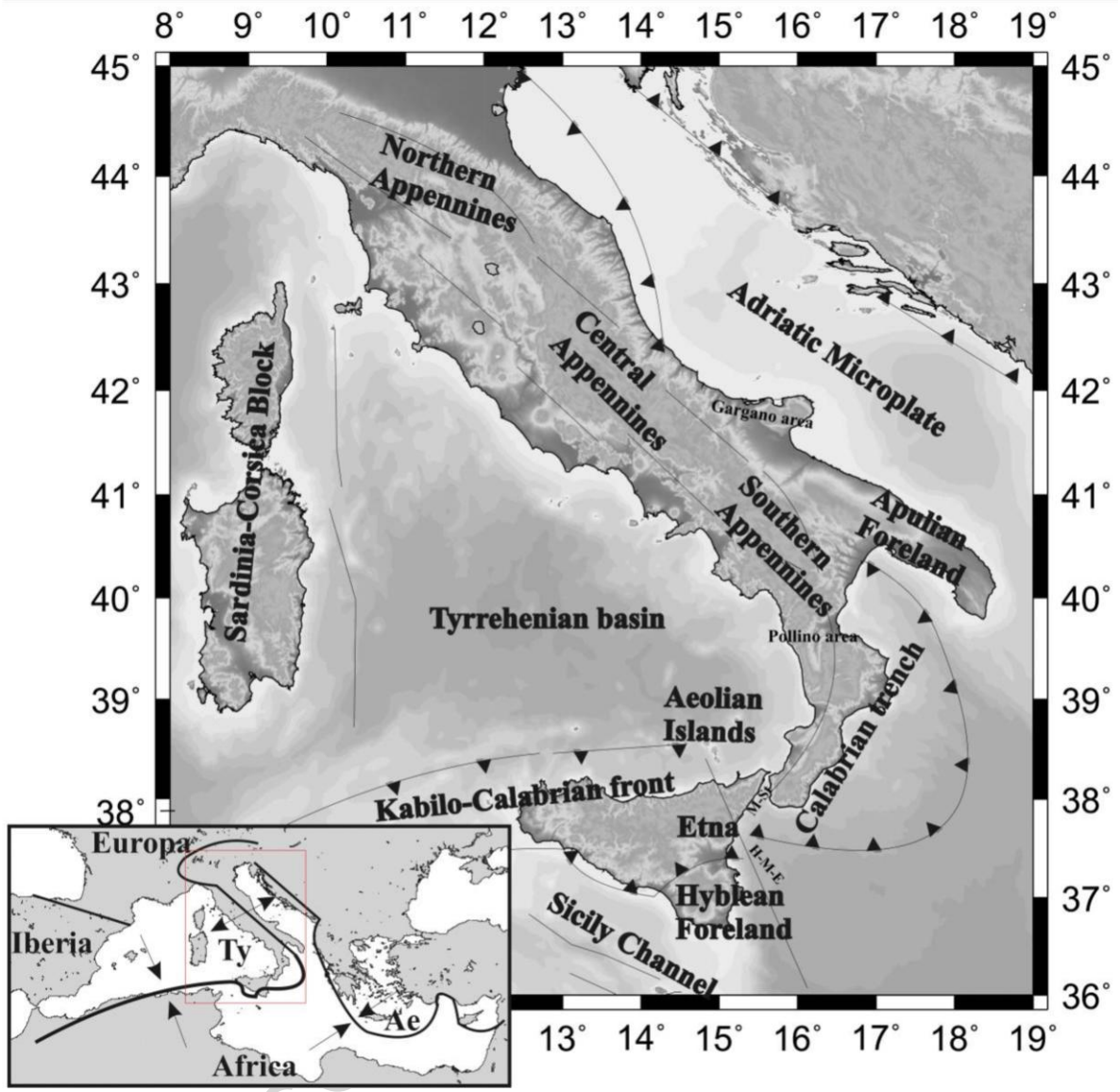

Figure 1

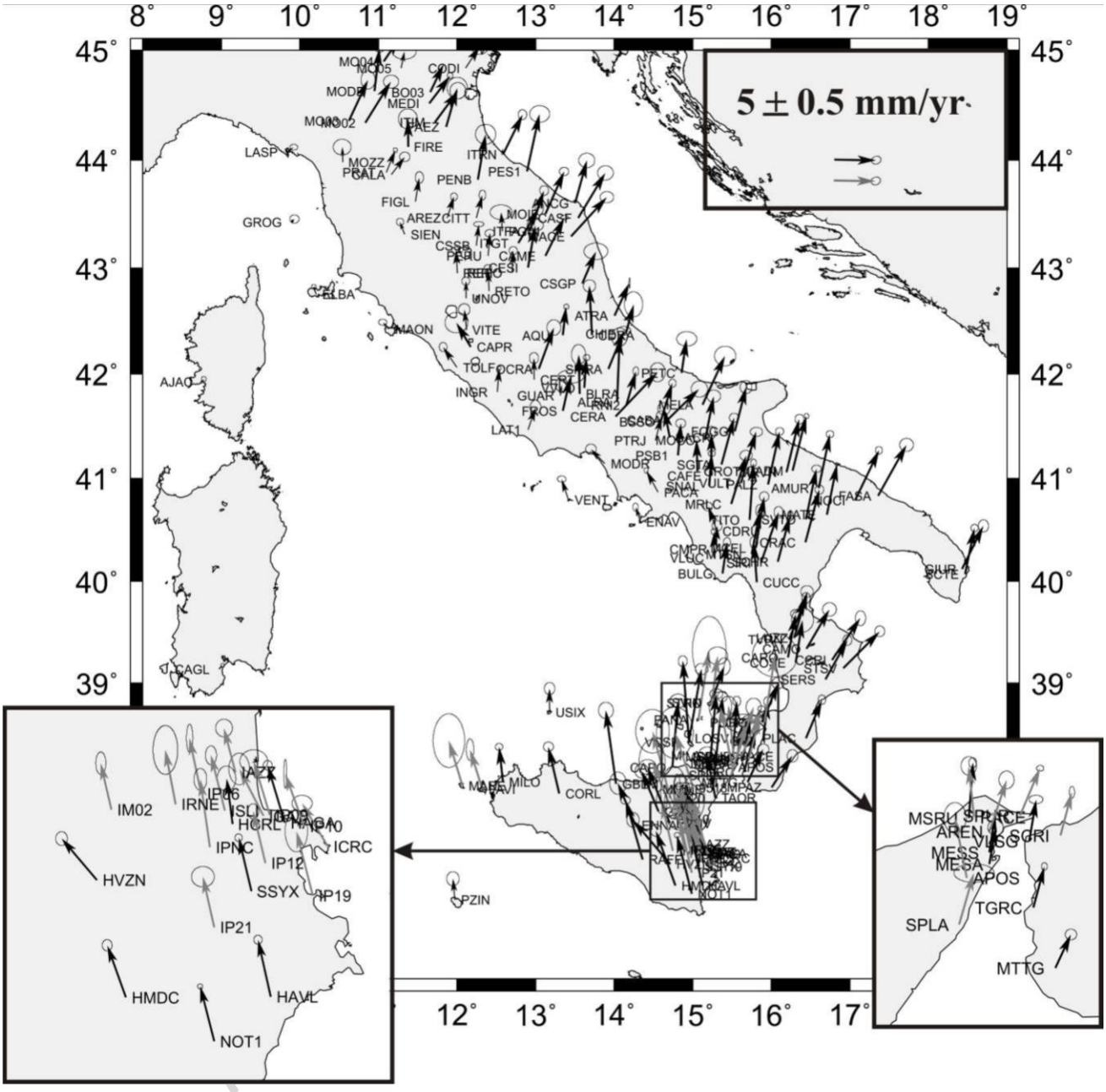

Figure 2

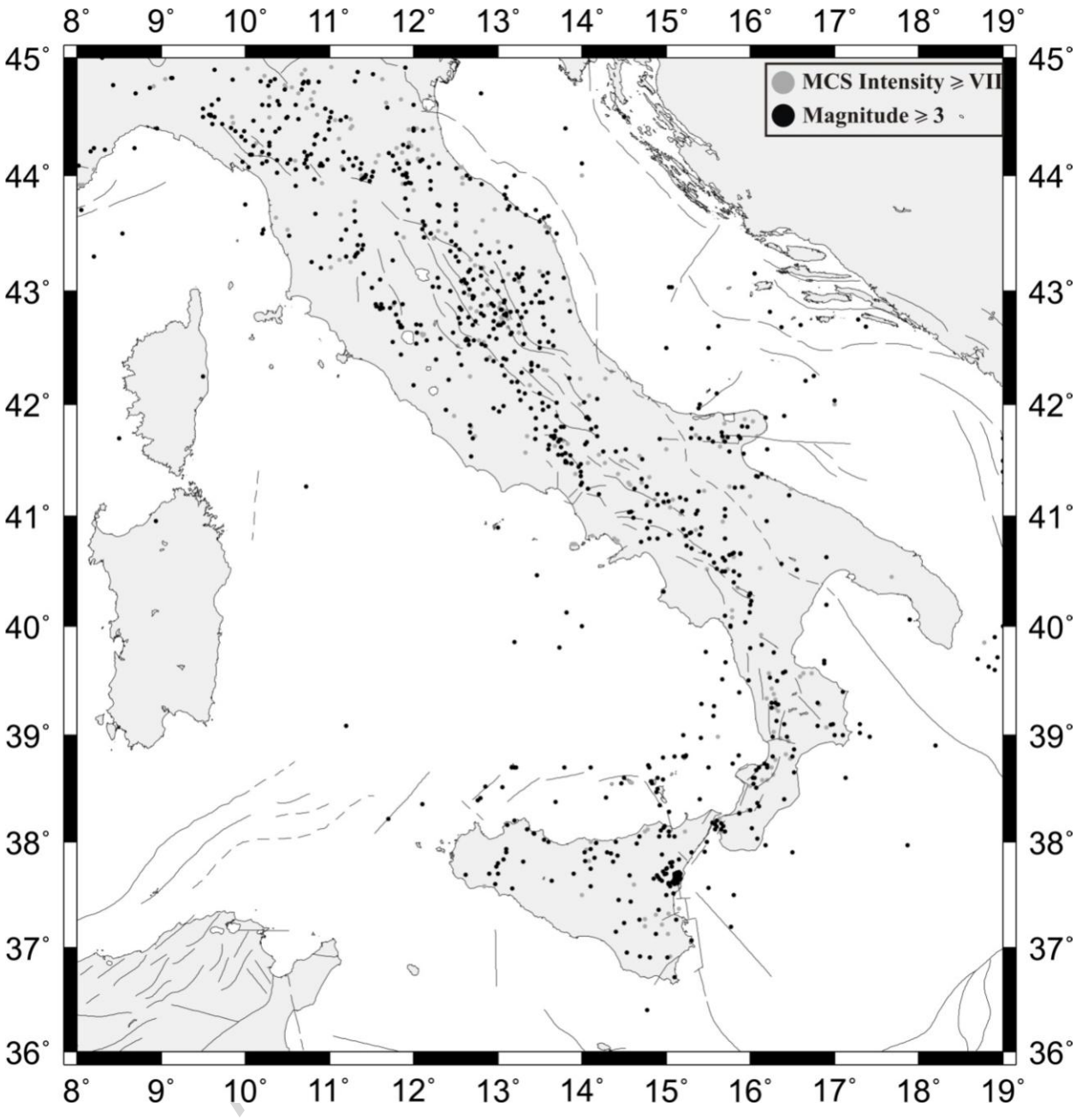

Figure 3

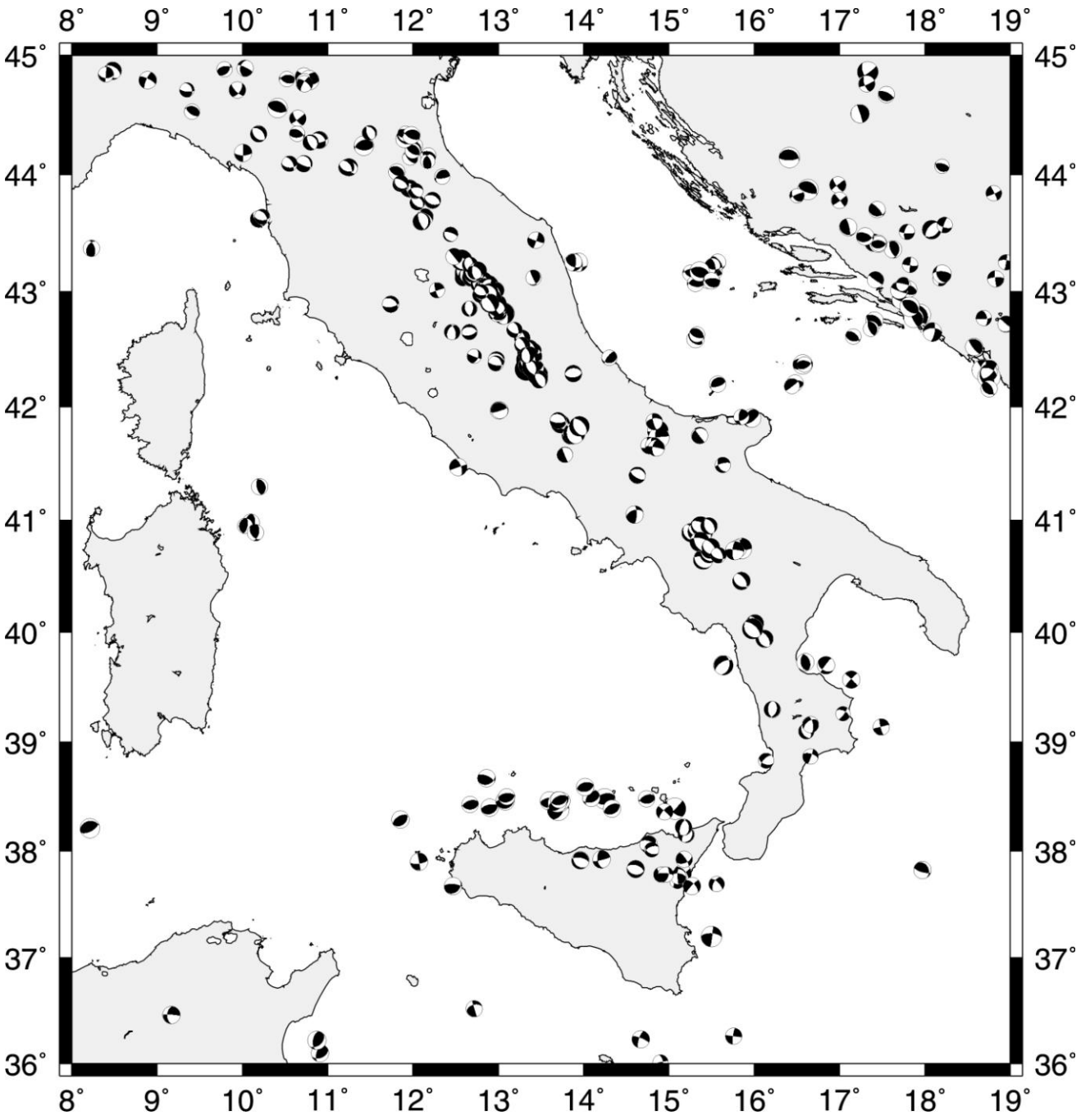

Figure 4

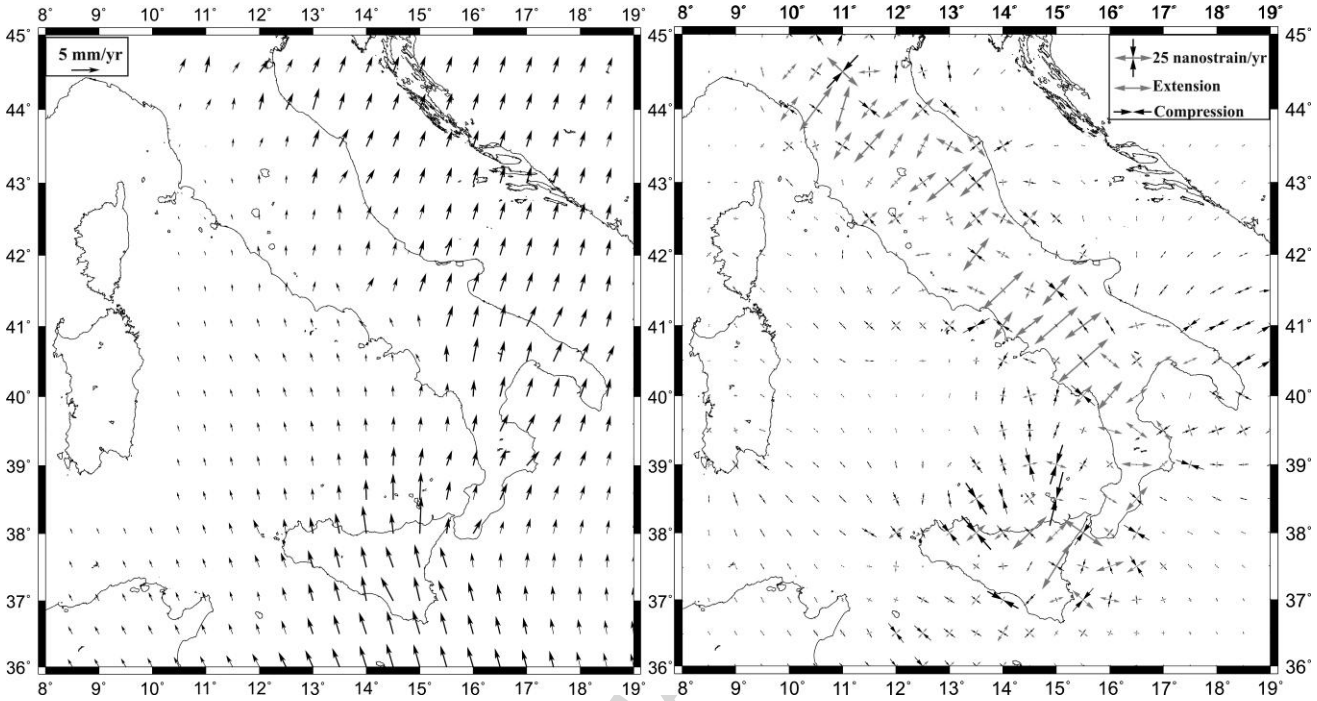

Figure 5

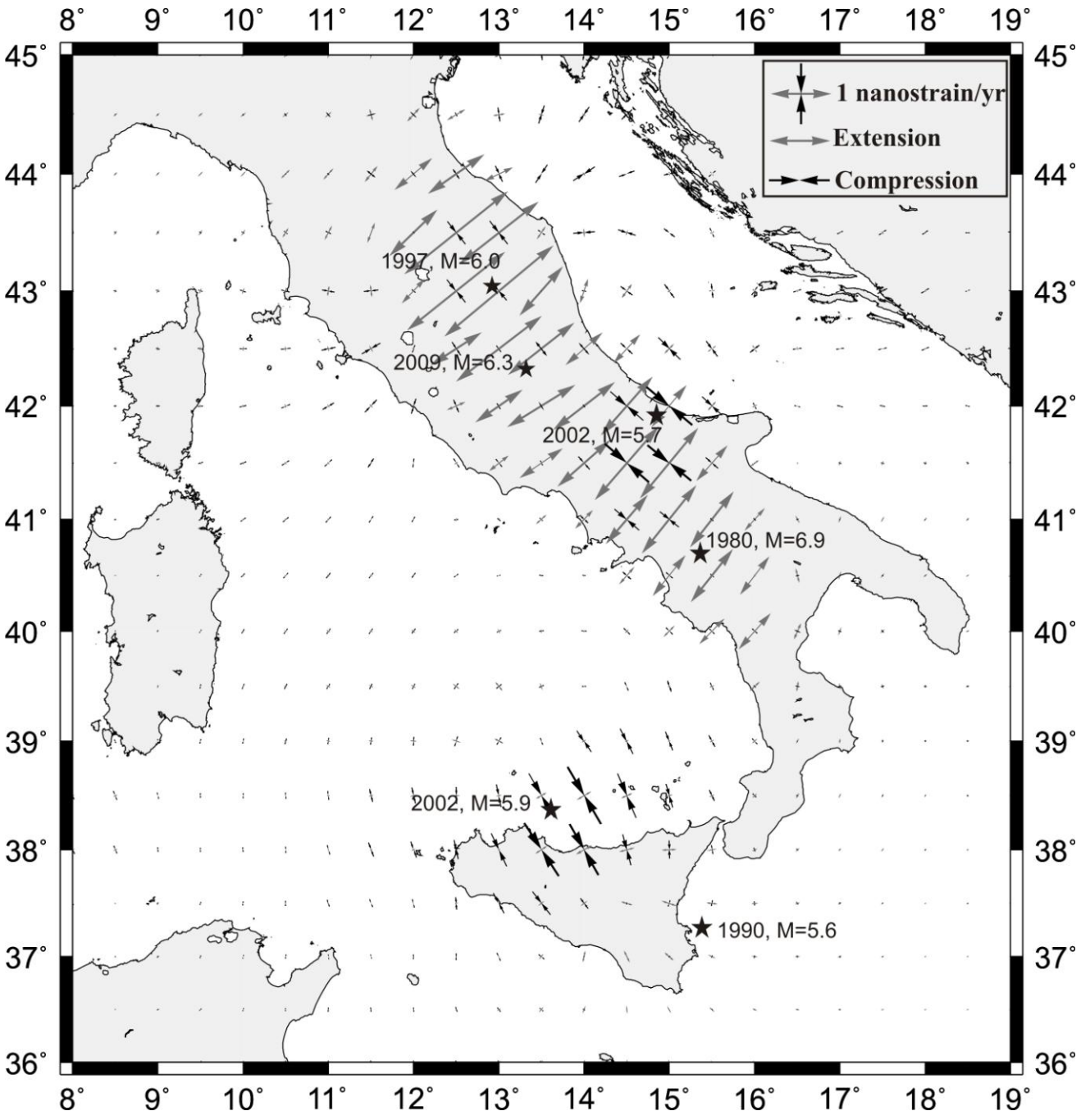

Figure 6

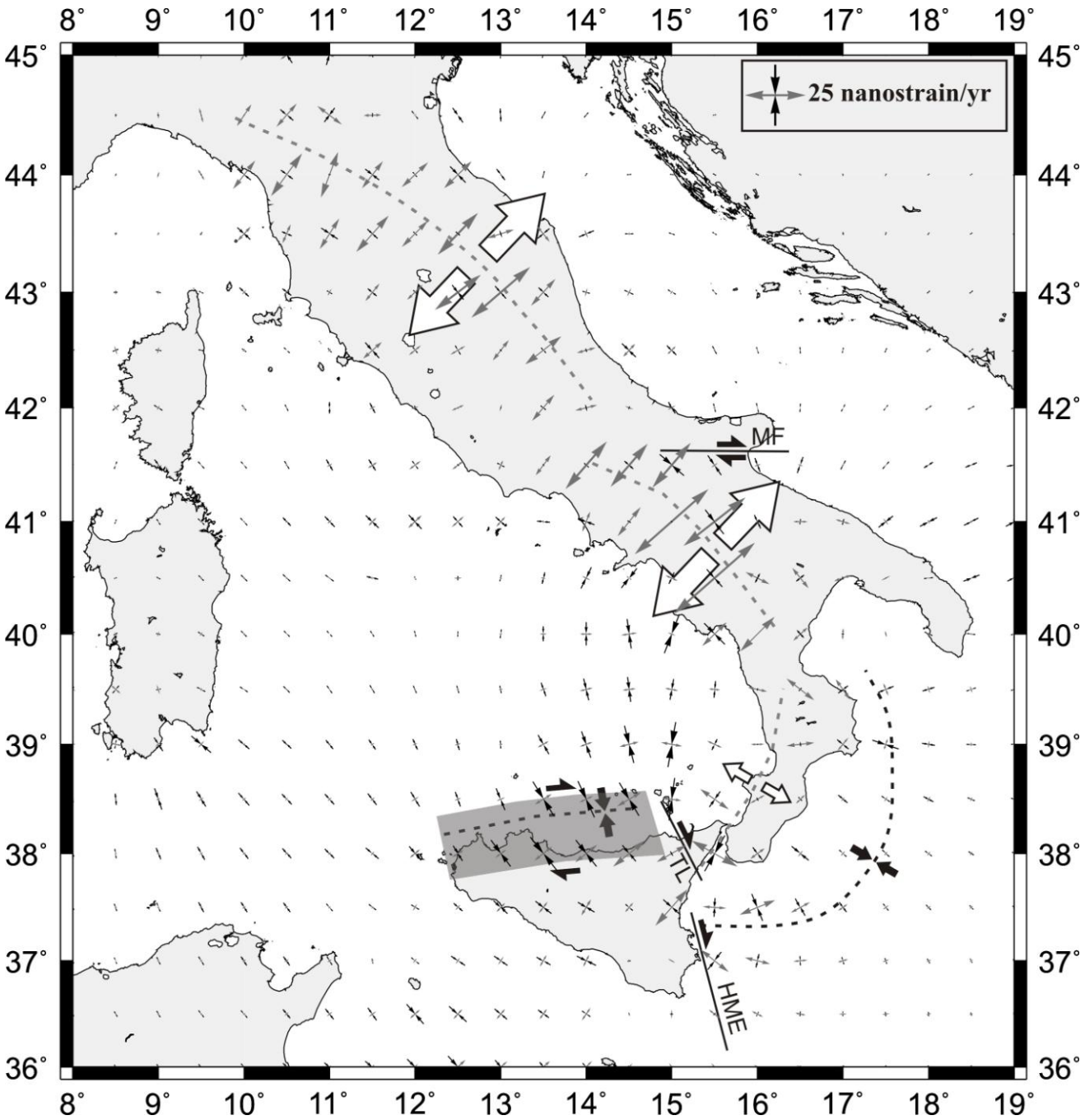

Figure 7

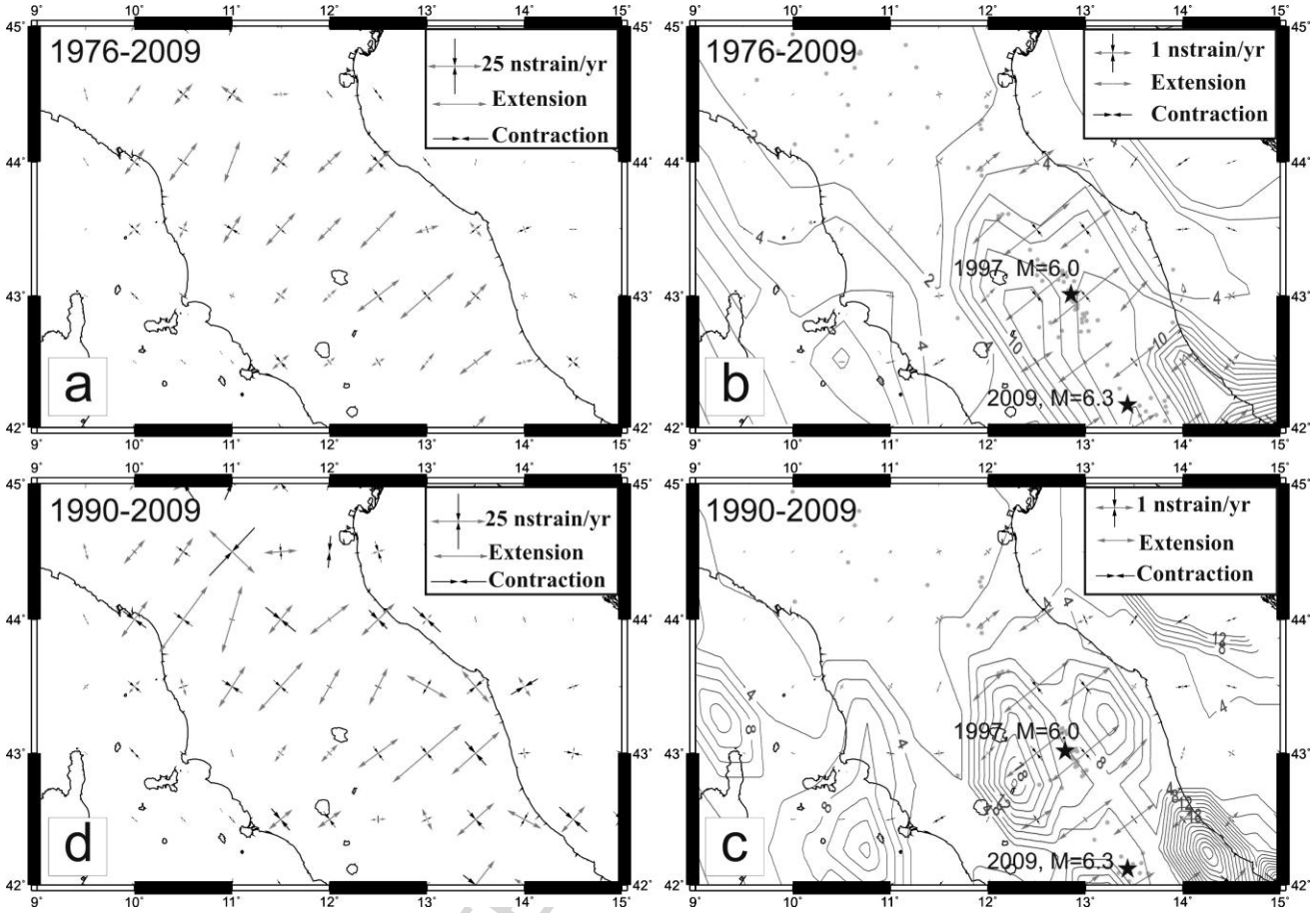

Figure 8

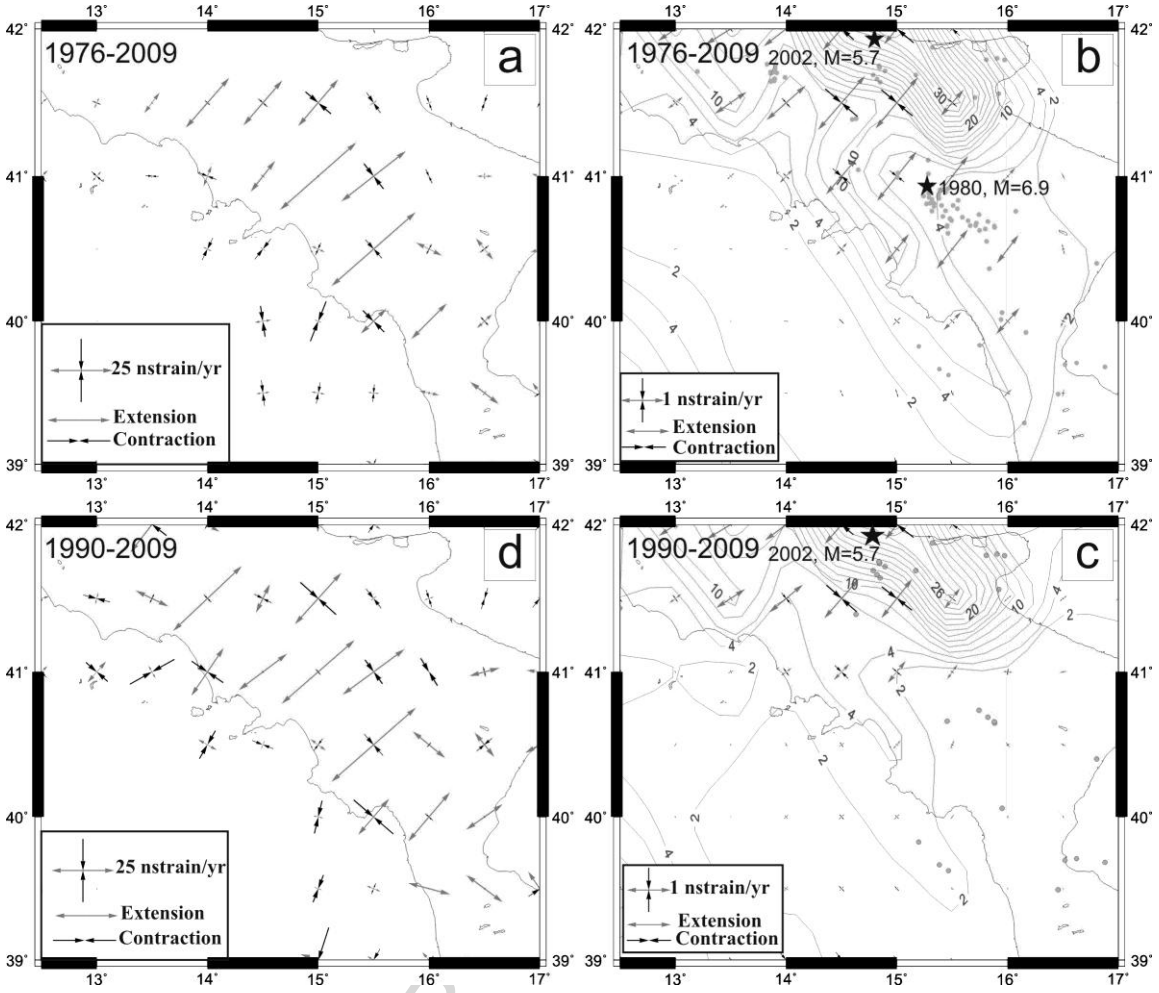

Figure 9

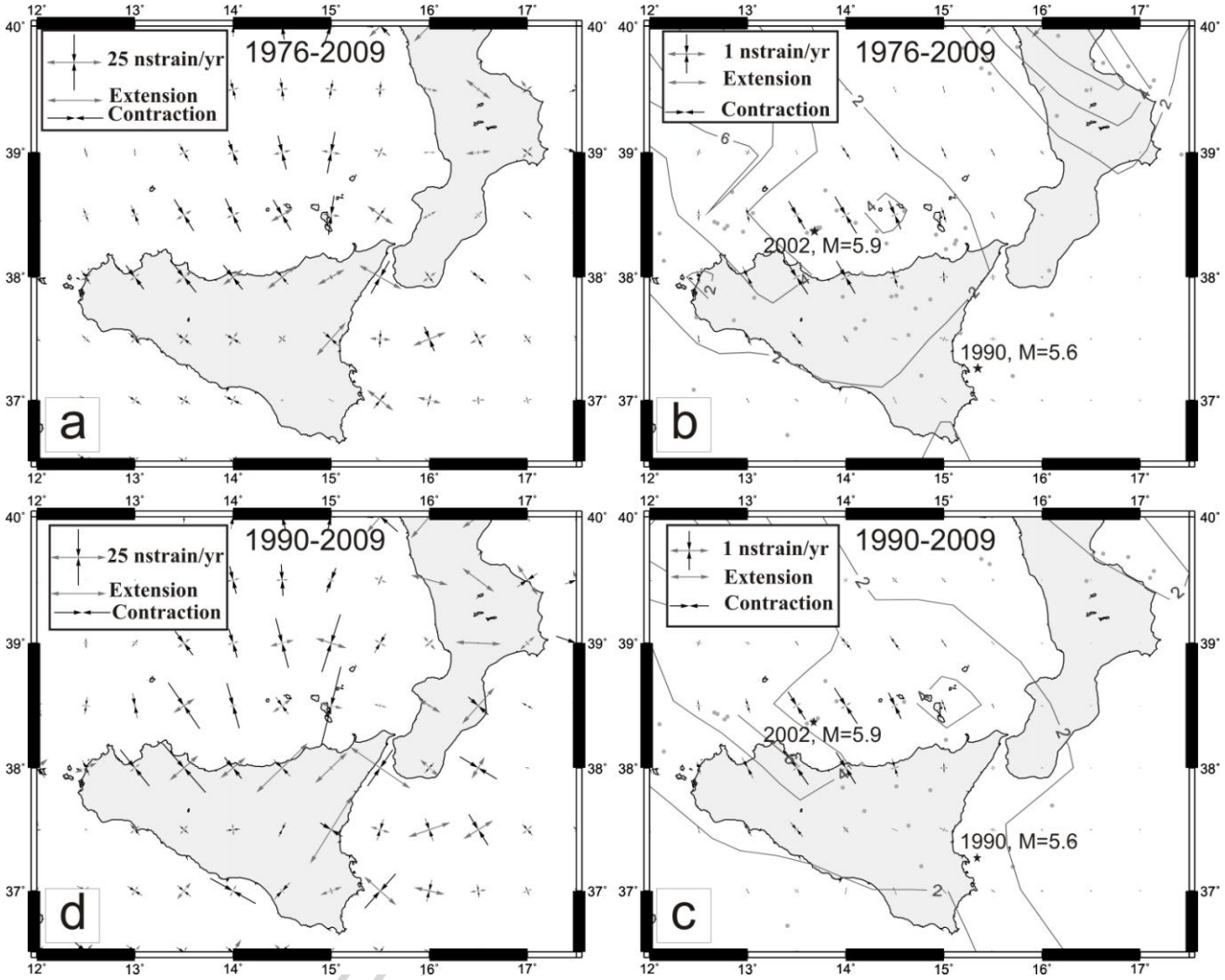

Figure 10

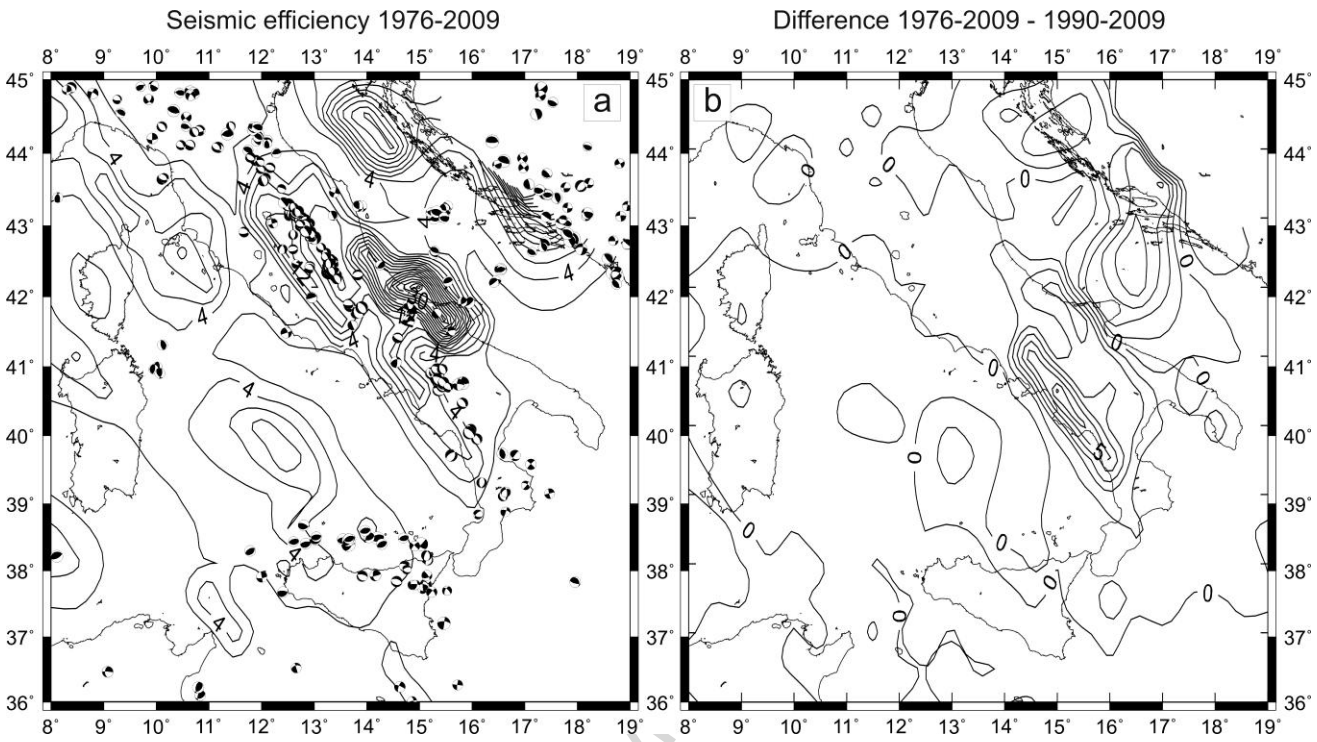

Figure 11

Highlights

- We processed GPS data for networks lying over the Italian peninsula
- We processed moment tensors of M≥4 earthquakes occurred in Italy since 1977
- We integrated both datasets to calculate the total strain rates
- We calculated the seismic efficiency over the peninsula for different periods
- Seismic efficiency and strain patterns highlight areas with higher seismic potential